ACS APPLIED MATERIALS & INTERFACES

Research Article

www.acsami.org

In-Plane Modulus of Singular 2:1 Clay Lamellae Applying a Simple Wrinkling Technique

Daniel A. Kunz,[†] Johann Erath,[†] Daniel Kluge,[‡] Herbert Thurn,[§] Bernd Putz,[†] Andreas Fery,*[,‡] and Josef Breu*[,†]

[†]Department of Inorganic Chemistry I, [‡]Department of Physical Chemistry II, and [§]Computing Center, University of Bayreuth, Universitätsstraße 30, D-95440 Bayreuth, Germany

Supporting Information

ABSTRACT: Knowledge of the mechanical properties of singular clay lamellae is of crucial importance for the optimization of clay−polymer nanocomposites. On the basis of controlled stress release, singular 2:1 clay lamellae show regular wrinkles on a deformable substrate. A subsequent two-dimensional Fourier transformation gives an in-plane modulus of the clay lamella of approximately 150 GPa. Only readily-available topographical atomic force microscopy is required for analysis rendering that fast and facile procedure generally applicable for nanoplatelet characterization.

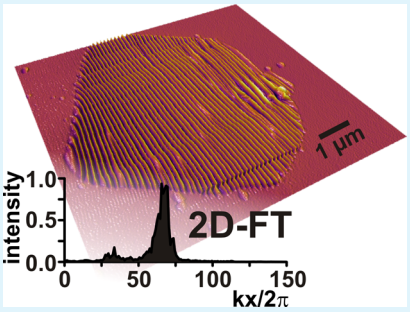

KEYWORDS: *nanomechanics, wrinkling, nanoplatelet, clay, nanocomposite, AFM*

INTRODUCTION

A plethora of nanocomposites contain clay platelets as functional compounds embedded in a variety of polymer matrixes. Besides electric,[1] fire-retardant,[2,3] and gas-barrier properties,[4,5] the most prominent function of clay fillers is mechanical reinforcement of nanocomposites.[6] Along that line, tremendous improvements of mechanical performance have been reported for ultrastrong, clay-based artificial nacre.[7,8]

In general, with fixed filler content, the performance of nanocomposites may be optimized by tuning four crucial factors regarding the clay filler: perfect texture, maximized aspect ratio, smart interface management, and excellent mechanical properties. The aspect ratio of layered 2:1 silicates may be easily modified for swelling clays like montmorillonite or hectorite by exfoliation or delamination,[9] which is fostered by the extensive intercalation chemistry. Contrary to swelling clays, structurally related nonswelling micas come with nonadjustable thickness of the platelets. As a consequence of the stronger interaction along the stacking direction, micas can, however, be obtained in crystals of appreciable thickness (>10 μm). The potential reinforcement of platy fillers, as given, e.g., by the Halpin-Tsai equations,[10] is determined by the aspect ratio and the ratio of the moduli of filler and matrix. However, clays, as any layered filler, are highly anisotropic, and the elastic constants differ by more than a factor of 3. While the elastic moduli of coarse-grained materials like mica have been determined, constants for completely delaminated singular clay lamellae, which are advantageous because of their maximized aspect ratio, would actually be needed. Usually bulk methodologies have been applied to obtain information on the mechanical properties of different types of clays,[11] ranging from compressibility measurements[12−15] to the extrapolation of data from epoxy−clay hybrids,[16] or acoustic measurements.[17,18]

Not surprisingly, the most reliable bulk elastic constants of 2:1 layered silicates have been obtained for coarse-grained micas via ultrasonic measurements,[19] inelastic neutron scattering,[20] and Brillouin scattering.[21,22] Results of computer simulations agree well with these experimental constants.[23] Knowledge about the elastic properties of swelling clay platelets that are actually used as fillers in nanocomposites because of the superior aspect ratio, however, is scarce. We recently determined, for the first time, the bending modulus of single hectorite tactoids, which represent semiordered crystals consisting of randomly oriented stacks of several individual 2:1 lamellae separated by hydrated interlayer cations. Atomic force microscopy (AFM)-based deformation measurements gave a significantly lower bending modulus for these hydrated clays than values reported for other types of nonswelling clays.[24] We proposed that the main reason for the surprisingly low modulus was the combination of hydration of interlayer cations and the decreased layer charge compared to that of micas in these swelling clays. Both effects lead to an increased contribution of shearing to bending deformations and therefore to a lower apparent bending modulus.[25] Because this effect will also be effective in composites, it will therefore reduce the efficiency of tactoids as filler material. In particular, tactoids thinner than 20 nm were found to be very flexible, and reinforcement of nanocomposites in a direction perpendicular

Received: April 24, 2013
Accepted: May 29, 2013
Published: May 29, 2013

to the platelets would be expected to be rather low. To calculate the reinforcement potential for real nanocomposites with more or less randomly oriented fillers, knowledge of the in-plane moduli of delaminated 2:1 lamellae, where no interlayer shearing can occur, is needed as well.

Such measurements, however, require a metrology that allows for orientation of singular 2:1 lamellae and that is able to cope with the compliant nature of such 1 nm thin nanoplatelets. In very demanding and impressive computer simulations of a single montmorillonite lamella by Suter et al.,[26] undulations caused by thermal fluctuations were observed, from which they were able to derive the in-plane modulus (230 GPa).

Analogously, it is possible to determine the in-plane modulus from forced undulations, which are also called wrinkles. The general idea of buckling-based metrology is the planar compression of a thin, stiff coating on a thicker, compliant substrate like poly(dimethylsiloxane) (PDMS). The wrinkling technique is well established for thin-film metrology[27,28] and in structure formation and patterning.[29−31] More recently, Reyes-Martinez et al. revealed in an intriguing investigation the elastic constants of rubrene microcrystals by the same technique.[32] Here we show that the wrinkling approach can even be transferred to single nanoplatelets of clays. The sought-after in-plane modulus of the nanoplatelet E_p depends on the characteristic wrinkling wavelength λ, on the platelet thickness h, and on Young's modulus E_s of the substrate:[33,34]

$$E_p = \frac{3E_s(1-\nu_p^2)}{(1-\nu_s^2)}\left(\frac{\lambda}{2\pi h}\right)^3 \quad (1)$$

where ν_p and ν_s refer to Poisson's ratios of nanoplatelet and substrate, respectively.

Simple topographical AFM imaging of the wrinkled platelets is sufficient to retrieve the in-plane modulus (Figure 1).

RESULTS AND DISCUSSION

Melt synthesis,[35−37] followed by long-time annealing, yielded sodium fluorohectorite ($Na_{0.5}Li_{0.5}Mg_{2.5}Si_4O_{10}F_2$, Na-hec) with lateral extensions of several micrometers and high intracrystalline reactivity.[38] This Na-hec spontaneously delaminates in water by osmotic swelling.[39] The van der Waals height of the silicate lamella deprived of hydrated counterions can be derived from the basal spacing of nonhydrated sodium hectorite to be 0.96 nm[37] (Figure 2).

A droplet of a diluted Na-hec suspension was placed onto a hydrophilized slab of PDMS that was uniaxially stretched with a customer-made apparatus (Figure S1, Supporting Information). After gentle drying and stress release, the sample was analyzed via AFM imaging. The results are shown in Figure 1. The hectorite lamella exhibited a uniformly wrinkled morphology, while the noncovered surface areas of the PDMS substrate remained featureless (Figure 1a). To recover the wavelength of the wrinkles, the recorded image was processed with a discrete two-dimensional Fourier transformation (2D-FT; see the Supporting Information for details). Figure 1b shows an intensity profile in reciprocal space along the axis of stress release (kx). It was integrated over a range of −5 to +5 ky values considering also the wrinkles that are slightly tilted away from 90°. The main peak corresponds to a wrinkling wavelength of 149 nm. Taking the same layer thickness as Suter et al.[26] and Kalo et al.[37] (0.96 nm) and applying eq 1 yielded an in-plane modulus of 143 GPa. Poisson's ratios of

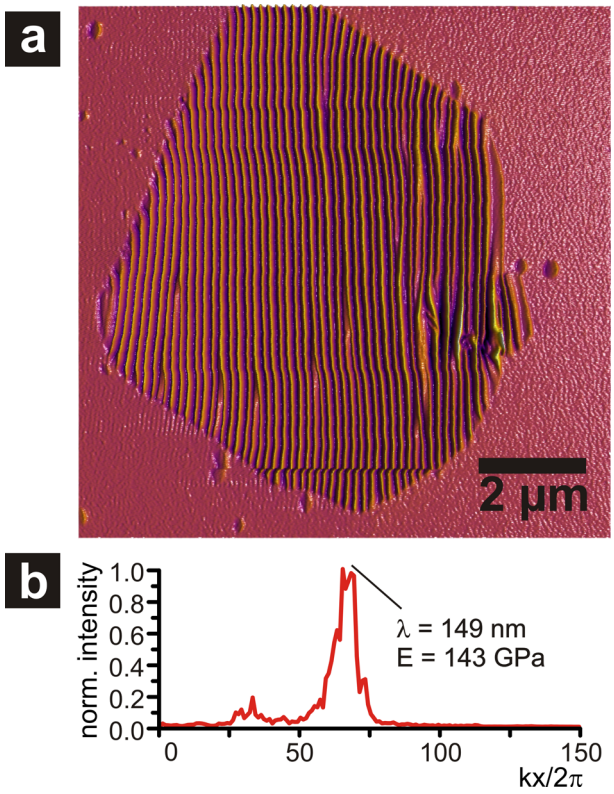

Figure 1. (a) AFM topographical image of a typical wrinkled Na-hec nanoplatelet on a featureless PDMS surface. (b) Normalized intensity profile after 2D-FT along kx, integrated over a range of −5 to +5 ky values, that considers also the wrinkles that are slightly tilted away from 90°. The peak represents a wrinkling wavelength of 149 nm corresponding to an in-plane modulus of 143 GPa.

0.5[40] and 0.3[41] for substrate and clay, respectively, were used. The Young's modulus of the PDMS substrate was measured to be 2.6 ± 0.1 MPa by applying a standard tensile test (see the Supporting Information). It has, however, been reported in the literature that low-molecular-weight species, e.g., non-cross-linked precursors, slowly migrate to the surface of PDMS and soften the local modulus.[42] Because this local surface modulus is actually the relevant modulus for the wrinkling metrology, it was additionally measured with a surface-selective metrology (colloidal-probe AFM[43−45]). While for a PDMS substrate aged for some months, the surface modulus was found to have decreased by 50%, for freshly prepared samples the bulk Young's modulus determined by tensile tests and the surface modulus determined by colloidal-probe AFM agree within experimental error. Therefore, it is strongly recommended to either use freshly prepared PDMS slabs (<2 weeks) for wrinkling metrology or determine the Young's modulus of the substrate's surface via colloidal-probe AFM.

In a recent work, Fu et al.[46] determined the minimum radius of curvature for a single clay lamella before failure to be 3 nm. That suggests that the deformations induced by wrinkling were clearly within the elastic regime. For instance, the radius of curvature of the wavelength observed in Figure 1 approximated by a sine wave with a wavelength of 149 nm and an amplitude of 18 nm yields a value of 31 nm (see the Supporting Information for details). A cross section of a wrinkled nanoplatelet (Figure S2,Supporting Information) shows a sine-wave profile, indicating that the clay lamella is completely adhered to the PDMS substrate by a strong cohesion.

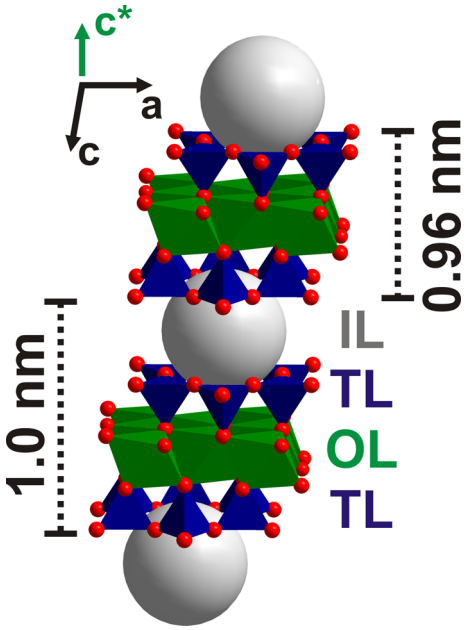

Figure 2. Structural representation of a mica crystal showing the two-dimensional, partially covalent Kagome network of basal oxygen atoms (TL) in combination with the trioctahedral layer (OL) connecting the two tetrahedral layers; the van der Waals height of the silicate lamella deprived of hydrated counterions is 0.96 nm.[26,37] The periodicity (basal spacing) of mica is, however, slightly larger (1.0 nm[48]) than the height of the 2:1 lamella because the structure represents a sandwich with the interlayer space (IL). The view is along the *b* axis; *c** represents the stacking direction of the crystal.

The FT peak indicated a uniform wrinkling wavelength throughout the whole lamella. The whole set of investigated platelets showed a uniform stiffness, suggesting that they were defect-free and are structurally homogeneous, with no clustering of isomorphous substitution. The latter statement is in line with a homogeneous charge density, as proven by a uniform intracrystalline reactivity of all interlayer spaces (ILs) reported earlier.[35,36,47]

Averaging the values of 16 hectorite monolayers yielded a mean in-plane modulus of 142 ± 17 GPa. The in-plane modulus found for a singular hectorite lamella is somewhat lower than those reported for in-plane moduli of various micas (average of C_{11} and C_{22} constants: 178.5 ± 1.5 GPa).[19−22] The mica structure can be regarded as a sandwich of relatively soft ILs and stiff silicate lamellae, resulting in a total basal spacing *d* of 1.0 nm[48] (Figure 2).

This sandwich construction might therefore lead to a certain stiffening of the bulk material,[49] as is known from light-weight construction materials.

Although it has been reported in the literature that hydrophilization of the PDMS substrate by HCl treatment does not affect the bulk modulus of PDMS significantly,[40] a minor change in the bulk modulus cannot be ruled out. A study with different durations of HCl treatment showed that the systematic error introduced would, however, be insignificant compared to possible errors related to uncertainties in the determination of the height of the platelets (Figure S4, Supporting Information). Averaging the values of five hectorite monolayers suspended on PDMS hydrophilized for 32 h instead of 16 h yielded a mean in-plane modulus of 154 ± 11 GPa.

The wrinkling wavelength is dependent on the strain, and eq 1 applied by us may be regarded as a first-order approximation. Because of the platelet thickness of <1 nm, the wrinkling metrology is pushed to its limit. Because the amplitude of the sine wave is directly related to the ratio of the Young's moduli of the substrate and clay platelet and the platelet height, a strain of >30% was necessary for a reliable measurement of the wavelength for these thin platelets. Unfortunately, no experimental values for the in-plane modulus of a single hectorite lamella are available in the literature to serve as a benchmark. We were, however, recently able to determine in-plane moduli of graphene oxide, chemically derived graphene, and CVD−graphene nanoplatelets by applying the very same method.[50] For these materials, independently measured reference values were available and could be reproduced with the wrinkling metrology with high accuracy. Moreover, in molecular dynamics simulations, spontaneous undulations were observed, and upon analysis of this buckling of clay nanoplatelets,[26] an in-plane modulus in fair agreement with our measurements could be derived (230 GPa).

When the strain-corrected models published by Rogers et al.[51] were applied, the effective wrinkling wavelength would be drastically enhanced, corresponding to a significantly higher in-plane modulus of 357 ± 42 GPa for hectorite platelets. However, our own preliminary results suggest that the strain dependency is significantly lower than those suggested by Rogers et al. Given the reasonable agreement with benchmark values available for other materials and with simulation results on clays, we refrain from applying corrections to eq 1.

The stiffness of the silicate lamella is assured by the two-dimensional, partially covalent Kagome network of basal oxygen atoms in combination with the trioctahedral layer connecting the two tetrahedral layers (Figure 2). Nevertheless, typical purely covalent two-dimensional networks like graphene still have an in-plane modulus approximately 8 times as high.[52]

Most of the moderate scatter of the wrinkling wavelengths is attributed to the slight tilt of the wavevector away from the axis of stress release. Another cause of scatter inherent to the wrinkling metrology is stochastically occurring local stress release by platelet breakage instead of wrinkling (Figure S3, Supporting Information), in particular, because additional edges are generated by the line defects, which can be attributed to defects in the platelet under tension (Poisson's expansion upon compression of the PDMS). It has been shown that these cracks do not directly influence the wrinkling wavelength.[31,53] These line defects, as well as the edges of the platelets, are, of course, expected to show lower moduli compared to undisturbed core areas, which is realized in a certain full width at half-maximum of the FT peak (Figure 1b).

CONCLUSION

The wrinkling method can easily be applied to any kinds of nanoplatelets, such as transition-metal sulfides and selenides,[54−56] layered double hydroxides, and, as already mentioned, graphene materials.[50,52] The great appeal of a simple approach requiring only standard and affordable AFM analytics renders the presented method a powerful tool that could be used as a quite ubiquitous, fast, low-cost, and facile standard method for large-scale mechanical characterization of nanoplatelets.[50]

■ ASSOCIATED CONTENT

Supporting Information

Materials and methods, additional analytical details, and supplementary figures and references. This material is available free of charge via the Internet at http://pubs.acs.org.

■ AUTHOR INFORMATION

Corresponding Author

*E-mail: andreas.fery@uni-bayreuth.de (A.F.), josef.breu@uni-bayreuth.de (J.B.). Phone: +49 921 55 2753 (A.F.), +49 921 55 2531 (J.B.). Fax: +49 921 55 2059 (A.F.), +49 921 55 2788 (J.B.).

Author Contributions

The manuscript was written through contributions of all authors. All authors have given approval to the final version of the manuscript.

Notes

The authors declare no competing financial interest.

■ ACKNOWLEDGMENTS

This work was supported by the German Science Foundation (Grant SFB 840). D.A.K. thanks the elite study program "Macromolecular Science" as well as the International Graduate School "Structure, Reactivity and Properties of Oxide Materials" within the Elite Network of Bavaria for ongoing support. Kai-Uwe Claussen and Andreas Schedl are gratefully acknowledged for helping with the PDMS tensile tests.

■ DEDICATION

Dedicated to Professor Wolfgang Bensch on the occasion of his 59th birthday.

■ REFERENCES

(1) Kurian, M.; Galvin, M. E.; Trapa, P. E.; Sadoway, D. R.; Mayes, A. M. *Electrochim. Acta* **2005**, *50*, 2125−2134.

(2) Schutz, M. R.; Kalo, H.; Lunkenbein, T.; Breu, J.; Wilkie, C. A. *Polymer* **2011**, *52*, 3288−3294.

(3) Schutz, M. R.; Kalo, H.; Lunkenbein, T.; Groschel, A. H.; Muller, A. H. E.; Wilkie, C. A.; Breu, J. *J. Mater. Chem.* **2011**, *21*, 12110−12116.

(4) Moller, M. W.; Kunz, D. A.; Lunkenbein, T.; Sommer, S.; Nennemann, A.; Breu, J. *Adv. Mater.* **2012**, *24*, 2142−2147.

(5) Kunz, D. A.; Schmid, J.; Feicht, P.; Erath, J.; Fery, A.; Breu, J. *ACS Nano* **2013**, *7*, 4275−4280.

(6) Goettler, L. A.; Lee, K. Y.; Thakkar, H. *Polym. Rev. (Philadelphia, PA, U. S.)* **2007**, *47*, 291−317.

(7) Tang, Z. Y.; Kotov, N. A.; Magonov, S.; Ozturk, B. *Nat. Mater.* **2003**, *2*, 413−418.

(8) Podsiadlo, P.; Kaushik, A. K.; Arruda, E. M.; Waas, A. M.; Shim, B. S.; Xu, J. D.; Nandivada, H.; Pumplin, B. G.; Lahann, J.; Ramamoorthy, A.; Kotov, N. A. *Science* **2007**, *318*, 80−83.

(9) Gardolinski, J. E. F. C.; Lagaly, G. *Clay Miner.* **2005**, *40*, 547−556.

(10) Halpin, J. C.; Kardos, J. L. *Polym. Eng. Sci.* **1976**, *16*, 344−352.

(11) Chen, B. Q.; Evans, J. R. G. *Scr. Mater.* **2006**, *54*, 1581−1585.

(12) Pawley, A. R.; Clark, S. M.; Chinnery, N. J. *Am. Mineral.* **2002**, *87*, 1172−1182.

(13) Pavese, A.; Ferraris, G.; Pischedda, V.; Mezouar, M. *Phys. Chem. Miner.* **1999**, *26*, 460−467.

(14) Smyth, J. R.; Jacobsen, S. D.; Swope, R. J.; Angel, R. J.; Arlt, T.; Domanik, K.; Holloway, J. R. *Eur. J. Mineral.* **2000**, *12*, 955−963.

(15) Faust, J.; Knittle, E. *J. Geophys. Res.: Solid Earth* **1994**, *99*, 19785−19792.

(16) Wang, Z. J.; Wang, H.; Cates, M. E. *Geophysics* **2001**, *66*, 428−440.

(17) Prasad, M.; Kopycinska, M.; Rabe, U.; Arnold, W. *Geophys. Res. Lett.* **2002**, *29*, 1172−1175.

(18) Vanorio, T.; Prasad, M.; Nur, A. *Geophys. J. Int.* **2003**, *155*, 319−326.

(19) Aleksandrov, K. S.; Ryzhova, T. V. *Bull. Acad. Sci. USSR, Geophys. Ser.* **1961**, *12*, 1165−1168.

(20) Collins, D. R.; Stirling, W. G.; Catlow, C. R. A.; Rowbotham, G. *Phys. Chem. Miner.* **1993**, *19*, 520−527.

(21) McNeil, L. E.; Grimsditch, M. *J. Phys.: Condens. Matter* **1993**, *5*, 1681−1690.

(22) Vaughan, M. T.; Guggenheim, S. *J. Geophys. Res.: Solid Earth* **1986**, *91*, 4657−4664.

(23) Collins, D. R.; Catlow, C. R. A. *Am. Mineral.* **1992**, *77*, 1172−1181.

(24) Kunz, D. A.; Max, E.; Weinkamer, R.; Lunkenbein, T.; Breu, J.; Fery, A. *Small* **2009**, *5*, 1816−1820.

(25) Whitney, J. M. *Structural Analysis of Laminated Isotropic Plates*; Technomic Publishing Company, Inc.: Philadelphia, PA, 1987; p 263.

(26) Suter, J. L.; Coveney, P. V.; Greenwell, H. C.; Thyveetil, M. A. *J. Phys. Chem. C* **2007**, *111*, 8248−8259.

(27) Stafford, C. M.; Harrison, C.; Beers, K. L.; Karim, A.; Amis, E. J.; Vanlandingham, M. R.; Kim, H. C.; Volksen, W.; Miller, R. D.; Simonyi, E. E. *Nat. Mater.* **2004**, *3*, 545−550.

(28) Bowden, N.; Brittain, S.; Evans, A. G.; Hutchinson, J. W.; Whitesides, G. M. *Nature* **1998**, *393*, 146−149.

(29) Lu, C. H.; Mohwald, H.; Fery, A. *Soft Matter* **2007**, *3*, 1530−1536.

(30) Genzer, J.; Groenewold, J. *Soft Matter* **2006**, *2*, 310−323.

(31) Pretzl, M.; Schweikart, A.; Hanske, C.; Chiche, A.; Zettl, U.; Horn, A.; Böker, A.; Fery, A. *Langmuir* **2008**, *24*, 12748−12753.

(32) Reyes-Martinez, M. A.; Ramasubramaniam, A.; Briseno, A. L.; Crosby, A. J. *Adv. Mater.* **2012**, *24*, 5548−5552.

(33) Huang, R. *J. Mech. Phys. Solids* **2005**, *53*, 63−89.

(34) Groenewold, J. *Physica A* **2001**, *298*, 32−45.

(35) Breu, J.; Seidl, W.; Stoll, A. J.; Lange, K. G.; Probst, T. U. *Chem. Mater.* **2001**, *13*, 4213−4220.

(36) Kalo, H.; Möller, M. W.; Ziadeh, M.; Dolejs, D.; Breu, J. *Appl. Clay Sci.* **2010**, *48*, 39−45.

(37) Kalo, H.; Milius, W.; Breu, J. *RSC Adv.* **2012**, *2*, 8452−8459.

(38) Stöter, M.; Kunz, D. A.; Schmidt, M.; Hirsemann, D.; Kalo, H.; Putz, B.; Senker, J.; Breu, J. *Langmuir* **2013**, 1280−1285.

(39) *Tonminerale und Tone: Struktur, Eigenschaften, Anwendungen und Einsatz in Industrie und Umwelt*; Jasmund, K., Lagaly, G., Eds.; Steinkopff Verlag GmbH & Co. KG: Darmstadt, Germany, 1993; p 110.

(40) Huang, H.; Chung, J. Y.; Nolte, A. J.; Stafford, C. M. *Chem. Mater.* **2007**, *19*, 6555−6560.

(41) Park, J. Y.; Lee, N. *J. Reinf. Plast. Compos.* **2007**, *26*, 601−616.

(42) Hillborg, H.; Tomczak, N.; Olah, A.; Schonherr, H.; Vancso, G. J. *Langmuir* **2004**, *20*, 785−794.

(43) Carrillo, F.; Gupta, S.; Balooch, M.; Marshall, S. J.; Marshall, G. W.; Pruitt, L.; Puttlitz, C. M. *J. Mater. Res.* **2005**, *20*, 2820−2830.

(44) Trenkenschuh, K.; Erath, J.; Kuznetsov, V.; Gensel, J.; Boulmedais, F.; Schaaf, P.; Papastavrou, G.; Fery, A. *Macromolecules* **2011**, *44*, 8954−8961.

(45) Gensel, J.; Dewald, I.; Erath, J.; Betthausen, E.; Muller, A. H. E.; Fery, A. *Chem. Sci.* **2013**, *4*, 325−334.

(46) Fu, Y. T.; Zartman, G. D.; Yoonessi, M.; Drummy, L. F.; Heinz, H. *J. Phys. Chem. C* **2011**, *115*, 22292−22300.

(47) Moller, M. W.; Hirsemann, D.; Haarmann, F.; Senker, J.; Breu, J. *Chem. Mater.* **2010**, *22*, 186−196.

(48) Brigatti, M. F., Guggenheim, S. *Micas: Crystal Chemistry & Metamorphic Petrology*; Mottana, A., Sassi, F. P., Thompson, J. B., Jr., Guggenheim, S., Eds.; Mineralogical Society of America: Washington, DC, 2002; p 1.

(49) Möller, M. W.; Handge, U. A.; Kunz, D. A.; Lunkenbein, T.; Altstädt, V.; Breu, J. *ACS Nano* **2010**, *4*, 717−724.

(50) Kunz, D. A.; Feicht, P.; Gödrich, S.; Thurn, H.; Papastavrou, G.; Fery, A.; Breu, J. *Adv. Mater.* **2012**, *25*, 1337−1341.

(51) Jiang, H. Q.; Khang, D. Y.; Song, J. Z.; Sun, Y. G.; Huang, Y. G.; Rogers, J. A. *Proc. Natl. Acad. Sci. U.S.A.* **2007**, *104*, 15607−15612.
(52) Lee, C.; Wei, X. D.; Kysar, J. W.; Hone, J. *Science* **2008**, *321*, 385−388.
(53) Lee, J. H.; Chung, J. Y.; Stafford, C. M. *ACS Macro Lett.* **2011**, *1*, 122−126.
(54) Coleman, J. N.; Lotya, M.; O'Neill, A.; Bergin, S. D.; King, P. J.; Khan, U.; Young, K.; Gaucher, A.; De, S.; Smith, R. J.; Shvets, I. V.; Arora, S. K.; Stanton, G.; Kim, H. Y.; Lee, K.; Kim, G. T.; Duesberg, G. S.; Hallam, T.; Boland, J. J.; Wang, J. J.; Donegan, J. F.; Grunlan, J. C.; Moriarty, G.; Shmeliov, A.; Nicholls, R. J.; Perkins, J. M.; Grieveson, E. M.; Theuwissen, K.; Mccomb, D. W.; Nellist, P. D.; Nicolosi, V. *Science* **2011**, *331*, 568−571.
(55) Zhou, K. G.; Mao, N. N.; Wang, H. X.; Peng, Y.; Zhang, H. L. *Angew. Chem., Int. Ed.* **2011**, *50*, 10839−10842.
(56) Zeng, Z.; Yin, Z.; Huang, X.; Li, H.; He, Q.; Lu, G.; Boey, F.; Zhang, H. *Angew. Chem., Int. Ed.* **2011**, *50*, 11093−11097.